We are IntechOpen, the world's leading publisher of Open Access books Built by scientists, for scientists

6,900
Open access books available

185,000
International authors and editors

200M
Downloads

Our authors are among the

154
Countries delivered to

TOP 1%
most cited scientists

12.2%
Contributors from top 500 universities



WEB OF SCIENCE™

Selection of our books indexed in the Book Citation Index in Web of Science™ Core Collection (BKCI)

Interested in publishing with us?
Contact book.department@intechopen.com

Numbers displayed above are based on latest data collected.
For more information visit www.intechopen.com



10

Ultrasonic Waves in Mining Application

Ahmet Hakan Onur[1], Safa Bakraç[2] and Doğan Karakuş[1]
[1]*Dokuz Eylul University*
[2]*Turkish General Directorate of Mineral Research and Exploration*
Turkey

1. Introduction

This chapter is aimed to introduce ways of beneficiation from ultrasonic waves in earth science, especially in mining practices. Since rocks are non-homogenous, elasto-plastic material, it has always been difficult to predict the behaviour of rock under any stress loaded environment. Unless removing uncertainties in the rock masses, designers can face to highly surprising and costly operational results in mining practices, so reducing the risk factor becomes vital element of underground constructions. To reduce risks may only be possible by knowing the surroundings where you work in very well. Sometimes it becomes costly to make the mining environment clear, so some practical methods have been trying to develop over years. One of them is acoustic methods based on the theory of elasticity. The elastic properties of substances are characterized by elastic module or constants that specify the relationship between stress and strain. The strains in a body are deformations, which produce restoring forces opposed to the stress. Tensile and compressive stresses give rise to longitudinal and volume strains, which are measured as unit changes in length and volume under pressure. Shear strains are measured by deformation angles. It is usually assumed that the strains are small and reversible, that is, a body resumes its original shape and size when the stresses are relieved. If the stress in an elastic medium is released suddenly, the condition of strain propagates within the medium as an elastic wave.

The principle of the ultrasonic testing method is to create waves at a point and determine the time of arrival at a number of other points for the energy that is travelling within different rock masses. The velocity of ultrasonic pulses travelling in a solid material depends on the density and elastic properties of that material. The quality of some rock masses is sometimes related to their elastic stiffness and rock mass structure, such that the measurement of ultrasonic pulse velocity in these materials can often be used to indicate their quality, as well as to determine their elastic properties. Travelling velocities of ultrasonic pulses are high in homogenous rock masses with high mechanical properties (UCS, tensile strength, cohesion, internal friction angle), which can be used as identification method of the quality of any rock structure. Some methods had been developed to measure rock diggability, stress distribution near a mine opening, bench blasting efficiency due to structural identification of rock masses by comparing the ultrasonic pulse travelling velocities in a reference sample with real in-situ measurements. In laboratory scale, available techniques and measurable rock mass properties are given in Table 1.

Non-destructive Methods	Crack Location	Thickness	Water Content	Hardness	Density	Reinforcement	Delimitation	Other
Acoustic Emission	■							
Electrical		■	■		■	■		
Electromagnetic		■	■			■	■	■
Nuclear	■	■	■		■	■		■
Ultrasonic	■	■				■	■	
Mechanical	■	■		■		■	■	■

Table 1. Non-destructive methods and applications (Moozar, 1993)

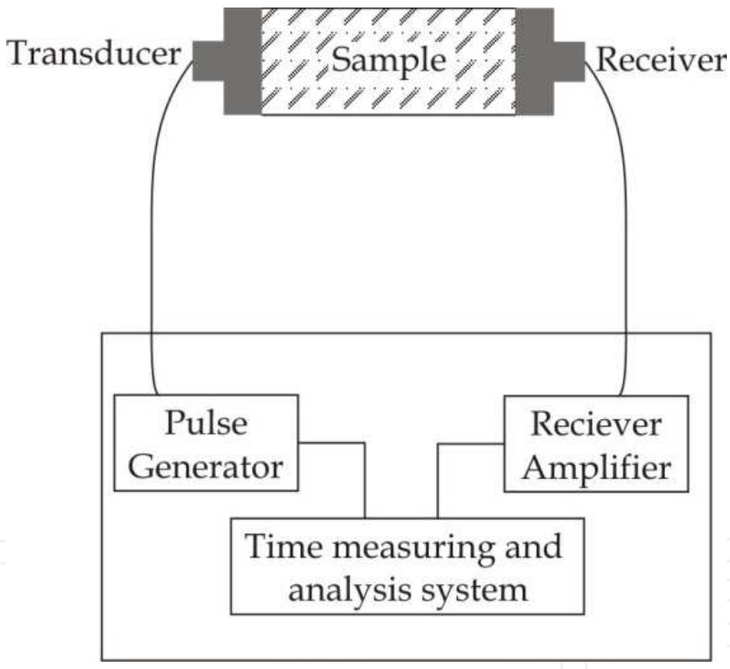


Fig. 1. Pulse velocity test (Malhotra & Carino, 1991)

Discontinuities and their dimensions within any material can be determined by the techniques given in Table 1 (Hasani et al.). There are four main measuring methods, namely; pulse velocity, pulse echo, resonant frequency and sonic tomography. Pulse velocity measures the time of an ultrasonic pulse within a material, hence finding the pulse velocity of the medium. The instruments used with this system include piezoelectric transducers, coupling agents, pulse generator, signal amplifier and an analyses system (Fig. 1.). The Pulse Echo system uses the transmission of low stress pulse energy to its sensor to delineate defects of material. The echoes received from defects are captured on a time domain

spectrum and their analysis locates the anomalies within the structure. The resonant frequency test defines dynamic property of a sample and in generally used in laboratory environments. An oscillator outputs vibrations, which is analysed into the materials transverse, longitudinal and torsional frequencies of the material. Sonic tomography analyses seismic P-wave velocities to image sections of a material. The idea behind the previous technique and the ultrasonic pulse velocity method is similar; however sonic tomography can use a large number of transmitters and receiver at the same time. Its sensivity allows this method to analyse between different anomalies within a structure and process a sectional view of a sample (Moozar, 1993).

There has been big development on measurement devices, since their first introduction by Leslie & Cheesman (1949). Then, measurement techniques pervaded in rock mechanic application given rise to ASTM D2845-08 Standard Test Method for Laboratory Determination of Pulse Velocities and Ultrasonic Constants of Rock. This test method describes equipment and procedures for laboratory measurements of the pulse velocities of compression waves and shear waves in rock and the determination of ultrasonic elastic constants of an isotropic rock or one exhibiting slight anisotropy.

This chapter is about to introduce a practical application of ultrasonic waves in marble industry. Miners working in the marble industry have always been interested in identifying structural weaknesses in marble blocks before they are cut in a marble quarry and transported to marble processing plants. To achieve this difficult task, several simple methods have been developed among miners but observation-based methods do not consistently provide satisfactory results. A nondestructive method developed for testing concrete could be used for this purpose. In this chapter, this simple method based on differences in ultrasonic wave propagation in different rock masses will be presented, and the test results performed both in the laboratory and a marble quarry will be discussed.

When ultrasonic testing is applied to marble blocks, its objective is to detect internal flaws that send echoes back in the direction of the incident beam. These echoes are detected by a receiving transducer. The measurement of the time taken for the pulse to travel from the surface to a flaw and back again enables the position of the flaw to be located. This ultrasonic testing technique was originally developed for assessing the quality and condition of concrete. One instrument used for this purpose is known as PUNDIT. The apparatus has been designed especially for field testing, being light, portable and simple to use. Simple correlations between concrete strength, concrete aggregate gradation, water-cement ratio and curing time have been analyzed using PUNDIT.

The possibility of identifying these structural defects using ultrasonic pulses will be discussed and results obtained from these measurements will be introduced in the scope of this chapter. The shape and size of any abnormality in a block can be determined by direct measurements taken from suitably spaced grids. It is important to find the exact position of the surface in marble blocks so that precautions can be taken before the cutting process starts. As stated before, if any discontinuity surface lies in the pulse path, the measured time corresponds to the pulse that follows the shortest path. This is important because any discontinuity causes a time delay compared with the travel time of pulses in homogenous blocks. This study concentrated on the relationship between structural discontinuities and

ultrasonic pulse travelling velocities in non-homogeneous marble blocks. Mathematical formulations were developed to find the exact locations of the surfaces that cause a separation during the cutting process. To verify the mathematical model explained above, a cubic homogenous marble block with a certain cut inside was prepared in laboratory. This chapter also covers the results obtained from model marble block in laboratory as well as the in-situ measurements obtained from industrial size marble blocks. Block subjected to testing of mathematical modelling in the marble plant was observed in detail before and after slice cut and results will be discussed.

2. Ultrasonic waves in mining application

There are two main mining applications of ultrasonic waves: one is to define the mechanical properties of intact rock and other is to define geological structures of the rock masses. There are several studies on determination of rock characterisation such as uni-axial compressive strength, static modulus of elasticity via non-destructive techniques especially after development of Portable Non-Destructive Digital Indicating Tester (PUNDIT) (Bray & McBride 1992, Green, 1991, ISRM, 1979, Mix, 1987, Vary, 1991, Chary et all, 2006, D'Andrea et all, 1965, Kahraman, 2007, Vasconles et all, 2008, Bakhorji, 2010, Khandelwala & Ranjithb 1996)

The other area of beneficiation of ultrasonic waves is to achieve rock mass classification based on rock mass structures. Several researchers had done work on indirect in-situ measurements to obtain practical data for the rock mass classification studies, since classical methods are expensive and time taking processes (Lockner, 1993, Galdwin, 1982, Karpuz & Pasamehmetoglu, 1997, Ondera, 1963).

There are some works reported on mineral processing industry about ultrasonic waves such as discharging feeding chutes, vibro-acoustics crushers, increasing shaking table performance, ore washing, milling, screening and optimizing bulb performance in flotation (Ozkan, 2004, Stoev & Martin, 1992, Asai & Sasaki, 1958, Kowalski & Kowalska, 1978, Nicol et all, 1986, Slaczka, 1987, Yerkovic et all, 1993, Djendova and Mehandjski, 1986).

Ultrasonic velocity measurements have previously proven valuable tool in measuring the development of stiffness of cement mixtures, so an engineered mine cemented paste backfill material were tested by ultrasonic wave and it is reported that measurements can be used as a non-destructive test to be correlated with other forms of laboratory testing (Galaa, et al. 2011). Grouted rock bolts are widely used to reinforce excavated ground in mining and civil engineering structures. A research was performed to find opportunities for testing the quality of the grout in grouted rock bolts by using ultrasonic methods instead of destructive, time-consuming and costly pull-out tests and over-coring methods (Madenga, et al., 2009, Zou, et al., 2010, Madenga, et al., 2009). A valuable work was performed by Lee, 2010 to predict ground conditions ahead of the tunnel face. This study investigates the development and application of a high resolution ultrasonic wave imaging system, which captures the multiple reflections of ultrasonic waves at the interface, to detect discontinuities at laboratory scale rock mass model. Another application of ultrasonic waves was introduced by Gladwin, 2011 to determine stress changes induced in a large underground support pillar by mining development at Mt Isa Mine. They introduced an ultrasonic stress monitoring device and compared the results with continuous strain recordings at a nearby

site. (Renaud V, et al., 1990) deals with the determination of the excavated damaged zone around a nuclear waste storage cavity using borehole ultrasonic imaging. This analysis is based on a method that is able to sound and image the rock mass velocity field. Another interesting work was published by (Jones, et al., 2010) to monitor and assess the structural health of draglines. They had announced that, by using ultrasonic waves and by studying both the diffraction pattern and the reflected waves, it is possible to detect and size cracking in a typical weld cluster. In the work of Deliormanli at al. 2007, laboratory measurements of P and S wave velocities of marbles from different origins were presented and their anisotropic performances at pressures up to 300 MPa were calculated and compared with the elastic properties.

3. Determination of discontinuities in marble blocks via a non-destructive ultrasonic technique

This ultrasonic testing technique was originally developed for assessing the quality and condition of concrete. One instrument used for this purpose is known as PUNDIT. The apparatus has been designed especially for field testing, being light, portable and simple to use. Simple correlations between concrete strength, concrete aggregate gradation, water-cement ratio and curing time have been analyzed using PUNDIT (Saad & Qudais, 2005). Several articles have been published on the subject of defining the mechanical properties of several different materials apart from rock by nondestructive test methods based on ultrasonic wave propagation (Dereman et al., 1998, Zhang et al, 2006).

There has been a rapid increase in the demand for natural materials to be used in construction engineering, interior decoration, and urban fitting. Over the years, there has been no shortage of quarried blocks, but problems have been encountered in providing sufficient numbers of high quality marble blocks. Blocks of commercial size are directly extracted from the massif. In the case of homogeneous rocks having constant features, structural discontinuities affect the marketability of the blocks. It is important to identify such abnormalities in the marble before the cutting process is performed in order to save money and time. The possibility of finding these structural defects using ultrasonic pulses has been studied, and promising results were obtained. This study concentrated on the relationship between structural discontinuities and ultrasonic pulse travelling velocities in non-homogenous marble blocks. Mathematical formulations were developed to find the exact locations of the surfaces that cause a separation during the cutting process.

3.1 Elastic constants and waves

The principle of the method is to create wave at a point and determine at a number of other points the time of arrival of the energy that is reflected by the discontinuities between different rock surfaces. This then enables the position of the discontinuities to be deduced. The basis of the seismic methods is the theory of elasticity. The elastic properties of substances are characterized by elastic moduli or constants, which specify the relation between the stress and strain. The strains in a body are deformations, which produce restoring forces opposed to the stress. Tensile and compressive stresses give rise to longitudinal and volume strains which are measured as the measured as the change in

length per unit length or change in volume per unit volume. Shear strains are measured as angles of deformations. It is usually assumed that the strains are small and reversible, that is, a body resumes its original shape and size when the stresses are relieved. If the stress applied to an elastic medium is released suddenly the condition of strain propagates within the medium as an elastic wave. There are several kinds of elastic waves:

In the longitudinal, compressional of P waves the motion of the medium is in the same direction as the direction of wave propagation. These are ordinary sound waves. Their velocity is given by (New, 1985):

$$V_{\mathrm{p}} = \left(\frac{k4\mu / 3}{\rho} \right)^{1/2} \tag{1}$$

Where ρ is density of the medium and k bulk modulus, μ shear modulus of the medium respectively. In the transverse, shear or S waves the particles of the medium move at right angles to the direction of wave propagation and the velocity is given by (Tomsett, 1976):

$$V_{\mathrm{s}} = \left(\frac{\mu}{\rho} \right)^{1/2} \tag{2}$$

If a medium has a free surface there are also surface waves in addition to the body waves. In the Rayleight waves the particles describe ellipses in the vertical plane that contains the direction of propagation.

Another type of surface waves the Love waves. These are observed when the S wave velocity in the top layer of a medium is less than in the substratum. The particles oscillate transversely to the direction of the wave and in a parallel to the surface. The Love waves are thus essentially shear waves.

The frequency spectrum of body waves in the earth extends from about 15 Hz to about 100 Hz; the surface waves have frequencies lower than about 15 Hz (Parasnis, 1994). For the method described in this study P waves are of importance as exploration tools. For the materials like concrete, marble necessary frequency range changes from 20 – 250 KHz.

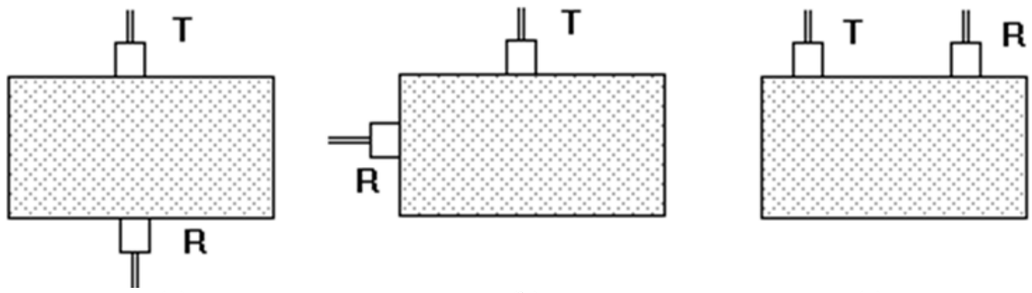
3.2 Application of pulse velocity testing

For assessing the quality of marble blocks from ultrasonic pulse velocity measurement, it is necessary to use an apparatus that generates suitable pulses and accurately measures the time of their transmission through the material tested. The instrument indicates the time taken for the earliest part of the pulse the transmitting transducer when these transducers are placed at suitable points on the surface of the material tested. The distance that the pulse travels in the material must be measured to determine the pulse velocity.

$$\text{Pulse velocity} = \frac{\text{Path length}}{\text{Transit time}} \tag{3}$$

Fig. 2. shows how the transducers may be arranged on the surface of the specimen tested. The transmission can either be direct (a), semi-direct (b) or indirect (c).

The direct transmission arrangement is the most satisfactory one since the longitudinal pulses leaving the transmitter are propagated mainly in the direction normal to the transducer face. The indirect arrangement is possible because the ultrasonic beam of energy is scattered by discontinuities within the material tested but the strength of the pulse detected in this case is only about 1 or 2 % of that defected for the same path length when the direct transmission arrangement is used. The purpose of the study was to develop a model in stone quarry so semi-direct and indirect transmissions were taken as the main measurement technique since it is sometimes very difficult to find free faces to place transducers on the production bench.



(a) (b) (c)

Fig. 2. Methods of propagating ultrasonic pulses

Pulses are not transmitted through large air voids in a material and, if such a void or discontinuity surface lies directly in the pulse path, the instrument will indicate the time taken by the pulse that circumvents the void by quickest route. It is thus possible to detect large voids when a grid of pulse velocity measurements is made over a region in which these voids are located. By using this behaviour, method can be used to test rock strata and provide useful data for geological survey work.

3.3 Laboratory works on simulated model

A concrete model was designed in laboratory to find out the behaviour of ultrasonic pulses travelling through a simulated discontinuity surface inside a concrete block. A wooden surface was settled in the block with the dimension shown in Fig. 3.

Before assessing the effects of simulated discontinuity on pulse velocity, first pulse velocity measurements made nearby simulated surface. This gives the real pulse velocity for prepared concrete block. For this purpose three direct measurements from three free surfaces were obtained. The result is given in Fig. 3.

For later use, a linear equation was set for the line shown in Fig. 4.

$$T = 2.52L - 3.39 \ (\mu s) \tag{4}$$

In equation 4, 2.52 is the slope of the direct line given in Fig. 4. and –3.39 is the value T takes when the length value L is equal to 0.

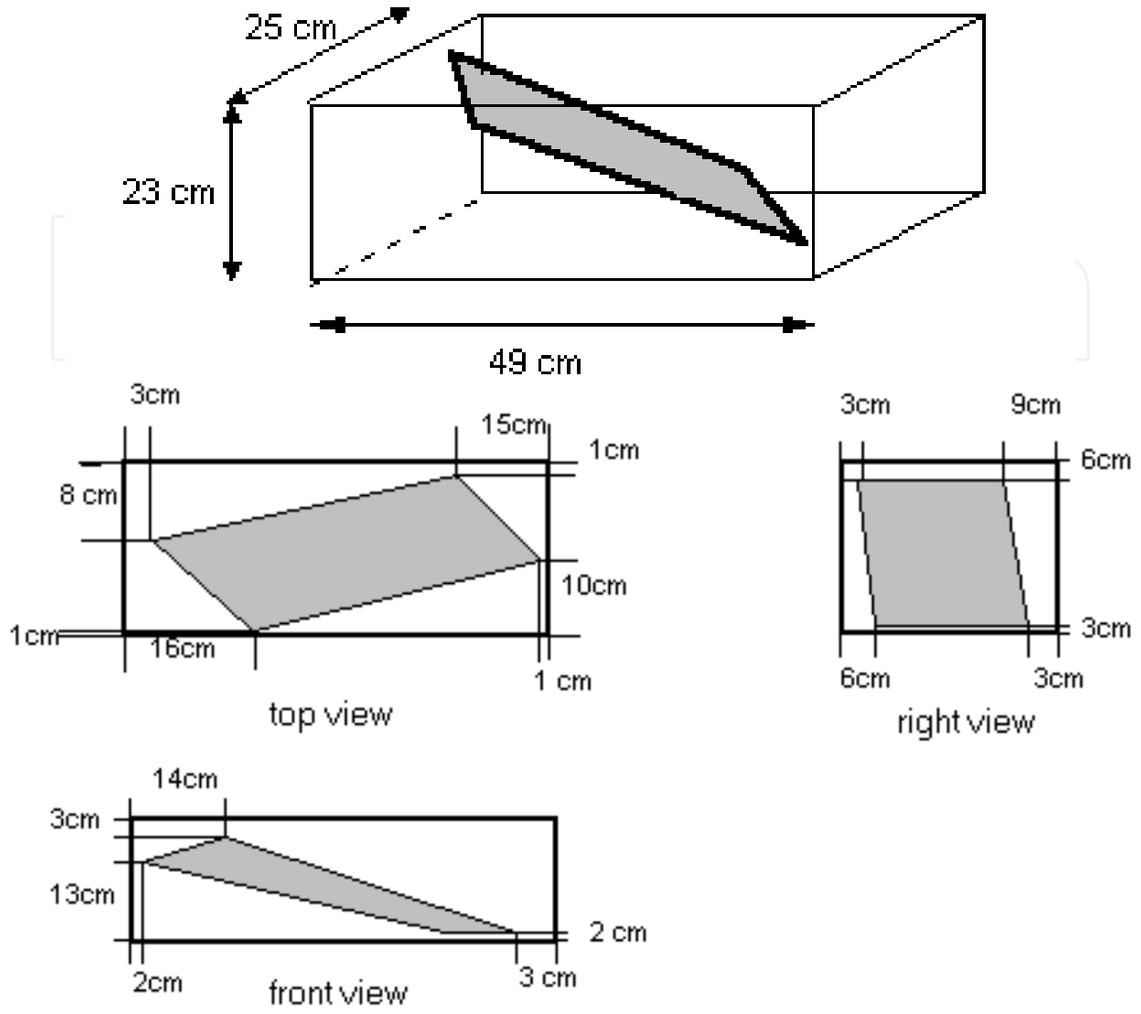


Fig. 3. Prepared concrete block and the dimension of the surface

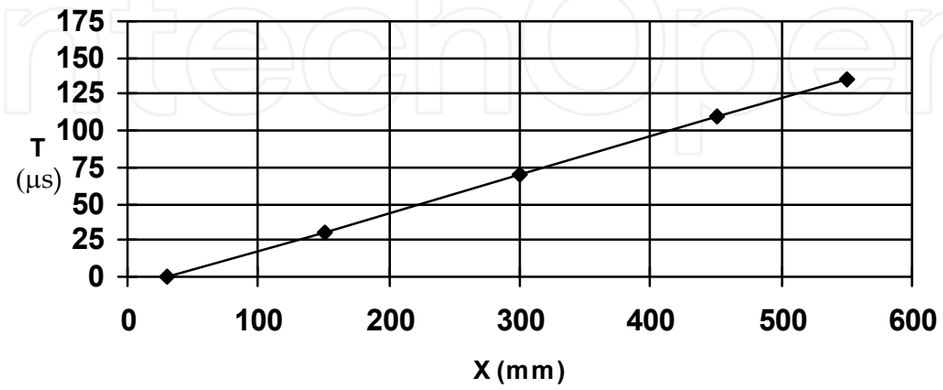


Fig. 4. Pulse velocity determination for homogenous concrete block

1	129.5	130.8	133.4	133.4	130.8	125.5	124.7	125.3	126.3
2	126.8	130.0	130.0	132.5	130.0	126.0	124.4	124.0	125.0
3	125.7	125.7	126.0	129.0	128.5	127.0	124.5	123.5	124.0
4	124.6	124.5	125.5	127.0	129.4	127.0	126.5	126.0	125.3
5	125.3	125.0	126.0	127.2	127.2	127.4	127.0	127.5	128.5
6	125.1	125.2	125.9	126.0	126.3	126.4	126.6	126.7	128.5
7	122.0	124.0	124.7	124.7	125.1	125.3	125.5	126.7	126.5
8	119.5	120.8	121.5	122.3	123.0	122.8	123.0	123.0	123.5
	1	**2**	**3**	**4**	**5**	**6**	**7**	**8**	**9**

Table 2. Transmission times taken from the right face of the concrete block (μs)

1	65.4	65.5	68.5	65.1	66.8	65.0	63.6	62.5	62.3	62.5	62.2	62.4	62.3	62.2	62.3	63.2	63.5	64.4	63.7
2	63.9	64.2	64.8	64.1	65.3	66.0	65.5	63.2	61.8	61.1	61.9	60.4	60.9	60.5	60.4	60.4	60.4	61.9	62.5
3	63.0	62.6	62.3	61.8	62.0	63.7	66.4	66.0	66.0	62.9	62.3	60.7	61.2	60.2	59.7	59.8	59.8	60.4	61.3
4	62.5	61.4	62.0	61.1	60.8	60.5	62.3	63.5	65.0	65.4	65.3	66.0	62.2	60.5	60.7	59.7	59.8	60.2	61.7
5	62.3	61.4	61.3	60.6	60.5	60.5	61.1	60.9	61.3	62.1	62.0	62.4	63.0	62.4	61.6	61.2	61.3	61.6	63.0
6	61.2	61.1	61.2	61.1	60.8	61.3	61.2	61.0	61.0	61.1	60.7	60.7	61.8	60.4	61.3	62.0	63.0	64.0	63.7
7	60.5	60.5	61.0	61.3	61.3	61.7	61.4	61.0	61.0	60.2	60.2	60.4	60.4	60.3	60.4	61.4	62.4	63.0	63.5
8	59.0	59.5	60.0	60.0	59.1	60.3	59.5	60.4	60.0	60.1	60.1	59.6	59.4	60.1	59.4	59.2	59.1	59.2	60.4
	1	**2**	**3**	**4**	**5**	**6**	**7**	**8**	**9**	**10**	**11**	**12**	**13**	**14**	**15**	**16**	**17**	**18**	**19**

Table 3. Transmission times taken from the front face of the concrete block (μs)

1	57.1	56.6	56.4	55.7	55.4	55.9	55.6	56.0	56.1	56.7	56.2	55.8	55.2	54.2	54.7	55.2	55.9	55.9	56.4
2	56.4	56.2	55.3	55.0	55.3	56.1	55.6	56.0	56.0	56.9	57.2	57.1	58.4	54.8	54.9	55.0	55.5	55.9	56.4
3	56.0	56.2	55.8	55.0	55.5	56.3	57.0	58.0	58.0	59.5	59.8	60.4	61.0	58.0	55.4	54.6	54.7	55.9	56.4
4	56.7	56.4	57.0	57.0	58.3	59.8	62.0	62.5	63.2	66.5	66.0	66.0	64.2	60.6	56.0	54.5	54.4	55.2	56.4
5	58.0	59.4	62.4	63.0	66.0	66.0	68.0	68.0	70.0	67.1	73.0	74.0	68.2	63.3	58.4	56.1	56.0	55.4	55.7
6	57.0	56.3	58.0	67.2	73.4	74.4	76.4	75.0	71.0	67.0	67.0	65.5	62.2	61.4	61.2	58.3	57.5	55.8	55.8
7	56.8	55.8	56.1	68.3	82.5	77.0	71.0	66.3	63.0	61.5	60.0	59.5	57.6	56.9	57.4	56.1	55.9	55.7	55.8
8	57.0	55.8	56.0	56.4	71.3	95.0	64.8	60.0	57.0	56.0	55.3	56.0	55.0	54.7	54.9	55.3	55.1	55.1	55.4
9	56.1	56.1	56.1	56.0	58.0	62.0	60.0	56.3	55.0	54.6	54.8	55.5	54.5	54.6	54.8	55.2	55.3	55.2	56.0
	1	**2**	**3**	**4**	**5**	**6**	**7**	**8**	**9**	**10**	**11**	**12**	**13**	**14**	**15**	**16**	**17**	**18**	**19**

Table 4. Transmission times taken from the top of the concrete block (μs)

Measurement of pulse velocities at points that are not affected by the simulated surface provides a reliable method of assessing the pulse velocity behaviour of the homogenous concrete block. It is useful to plot a diagram of pulse velocity contours from the result obtained since this gives a clear picture of the extent of variations. It should be appreciated that the path length can influence the extent of the variations recorded because the pulse velocity measurements correspond to the average quality of the concrete. When an ultrasonic pulse travelling through concrete meets a simulated surface, there is a negligible transmission of energy across this interface so that any air-filled

cracks or void directly between the transducers will obstruct the direct beam of ultrasound when the void has a projected area larger than the area of the transducer faces. The first pulse to arrive at the receiving transducer will have been diffracted around the periphery of the defect and the transit time will be longer than in similar concrete with no defect.

In order to detect the simulated surface, pulse velocity measurements were performed over three different directions of concrete block with a grid of 2.5 cm x 2.5 cm and results are given in Table 2, 3, 4.

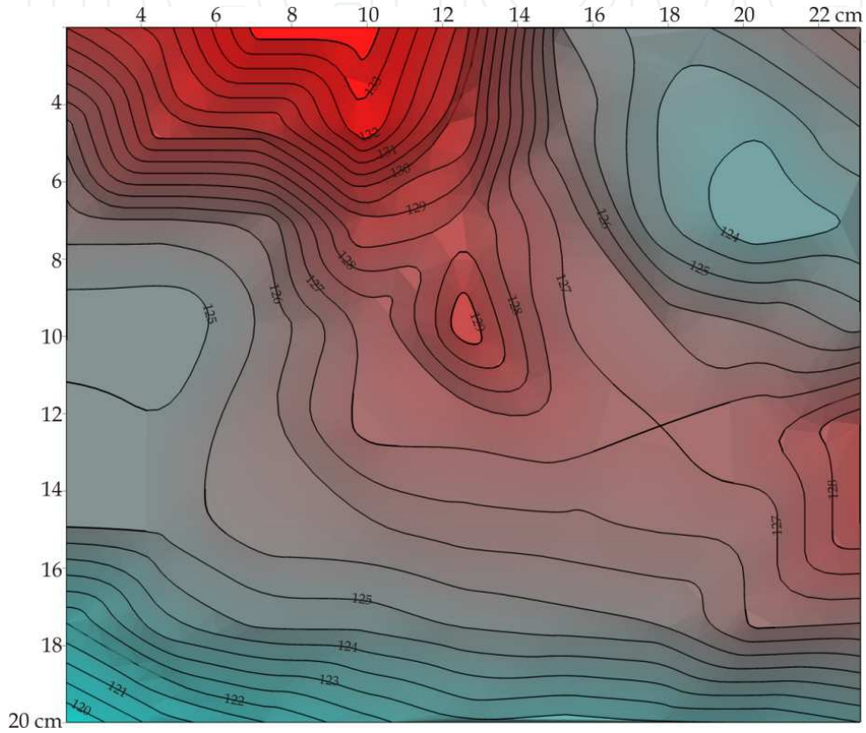


Fig. 5. Contour plotting of transmission times (μs) taken from right face

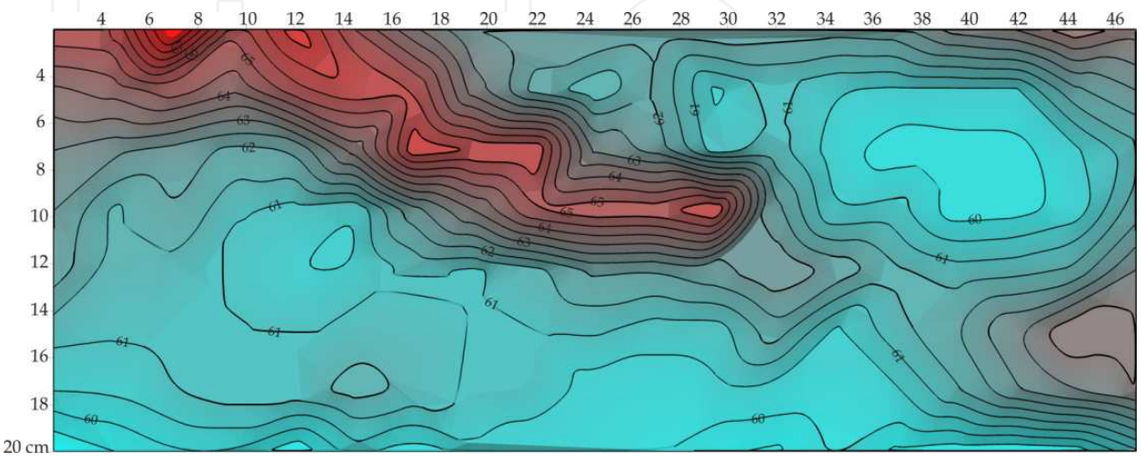


Fig. 6. Contour plotting of transmission times (μs) taken from front face of the model

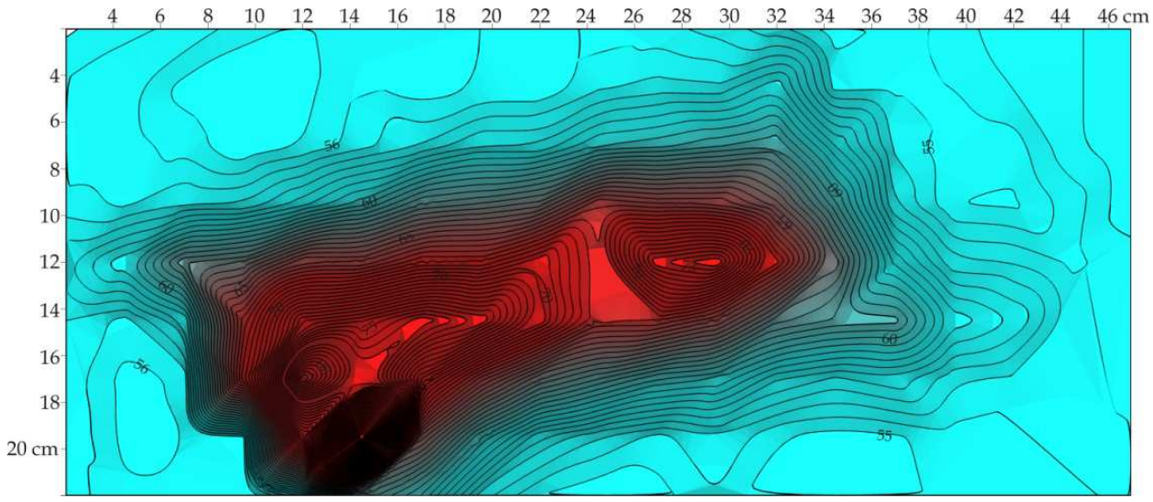


Fig. 7. Contour plotting of transmission times (μs) taken from top of the model

As shown in Fig. 5., Fig. 6. and Fig. 7., it is possible to detect the size and position of the simulated surface. Such estimates are more reliable if the discontinuity surface has a well-defined boundary surrounded by uniformly dense concrete.

3.4 Modeling the boundary of discontinuities

The shape and size of any abnormality in a block can be determined by direct measurements taken from satisfactory grids. It becomes important to find the exact position of the surface in marble blocks so that to take all precautions before cutting process starts. As stated before, if any discontinuity surface lies in the pulse path, the measured time belongs to the pulse that follows the shortest path. This is important because it causes a time delay comparing to travel time of pulses in homogenous blocks. This case is shown in Fig. 8.

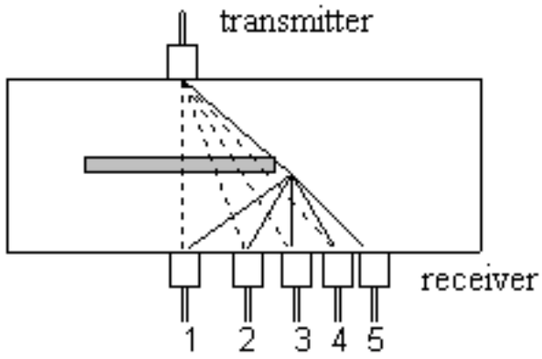


Fig. 8. The cause of time delay of pulses.

Before doing any measurement, pulse velocity behaviour of homogenous material must be obtained as discussed in laboratory work. By doing so, it becomes possible to estimate pulse travel time if no abnormality exists in the block. It is necessary to measure direct distance between transmitter to receiver in order to estimate travel time of pulses. The pulse velocity measuring device gives the minimum travelling time between two points. The pulse

velocity is obtained by dividing the path length to transit time. There will be a difference between the measured pulse velocity and the velocity obtaining from equation 3 by applying path length L in the formula. This difference is an indicator of a time delay caused by longer travelling distances due to obstacle in the pulse travel path (dashed lines in Fig. 8.). The time delay will be used later to find the correct position of surface in 3D.

Fig. 9. explains the situation clearly. In this figure, there are two types of curves in the graphics. The linear one represents the direct distance from transmitter to receiver; the parabolic one represents the longer path of pulses following the boundary of discontinuity. Both figures can be obtained from the type of measurement so that receiver moves away from position 1 to position 7 while transmitter stays stable.

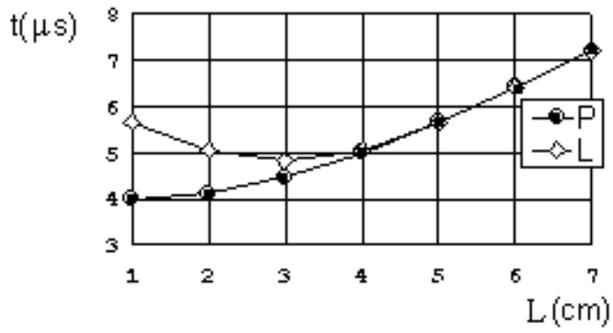


Fig. 9. The difference between direct distance and the pulse travel distance.

The first curve in Fig. 9 is the distance obtained from pulse travel times (shown as L in Fig. 9.) from receiver, the second one is the actual distance (shown as P in Fig. 9.) according to receiver position from 1 to 5. There has been a wide opening between two lines that shows the position of receiver 1 is away from the discontinuity surface. While the receiver moves along a line with equal distance from position 1 to 5 the gap between two lines narrows steadily. This behaviour gives a very important clue about the boundary of the surface. In the second region of the graph started from receiver position 5 to 7, two lines meet and behave in the same way. Because, at receiver position 5 the modelled surface has been passed that indicates there is no surface between transmitter and receiver. This kind of work defines the boundary in longitudinal location (s) but not in vertical one. As shown in Fig. 10. discontinuity can be at any position of (h) that is the vertical distance of the surface from top of the block.

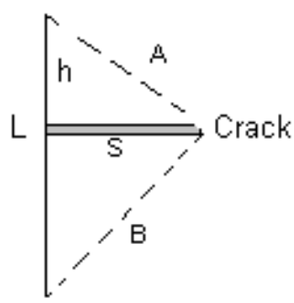


Fig. 10. Pulses moving around the crack

Lets take s as the length of crack, h is the vertical distance from surface, A + B is the path of pulse travelling from transmitter to receiver and L is the shortest distance between two probs. The pulse travels the distance A + B instead of L.

$$Ls = A + B \tag{5}$$

Some simple linear algebra can be used to obtain h and s those are the correct places of the boundary of discontinuity.

$$S^2 = A^2 - h^2 \tag{6}$$

$$S^2 = B^2 - (L-h)^2 \tag{7}$$

$$A^2 - h^2 = B^2 - (L-h)^2 \tag{8}$$

$$A^2 - B^2 = h^2 - (L-h)^2 \tag{9}$$

$$(A+B).(A-B) = h^2 - (L-h)^2 \tag{10}$$

$$A - B = \frac{h^2 - (L-h)^2}{Ls} \tag{11}$$

$$A = \frac{h^2 - (L-h)^2}{2.Ls} + \frac{Ls}{2} \tag{12}$$

$$S = \sqrt{\frac{h^2 - (L-h)^2}{2.Ls} + \frac{Ls}{2} - h^2} \tag{13}$$

Equation 13 is a function of vertical distance h. In this formula both s and h are unknowns. The purpose of all formulations above is to define h and s. In equation 13, if h changes from 0 to L and plotted, Fig. 11. can be obtained. In this process only the measurements that can be obtained are directly measured L, A+B that is estimated from the linear equation set before the homogenous material.

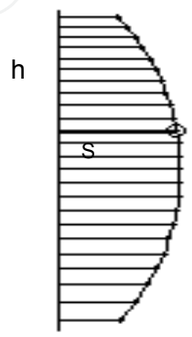


Fig. 11. The curve that shows possible path obtained from a single measurement.

When the receiver moves to position 2 in Fig. 12., the same measurements are made to plot second curve. Both figures are combined to obtain an intersection point that gives the correct position of the boundary, in another saying h and s can be determined (Fig. 12.).

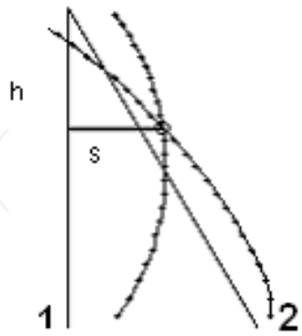


Fig. 12. The combined curves giving h and s

Obtaining h and s is very important because if the receiver moves in four different directions that mean four different h and s can be obtained in different directions. In common, receiver moves in such a way that enables us to find the exact shape of boundary of the discontinuity in 3D.

Finding h and s values are a time taken process so a computer program has been written to analyse and to plot the entire finding. For better understanding, Fig. 13. must be explained first.

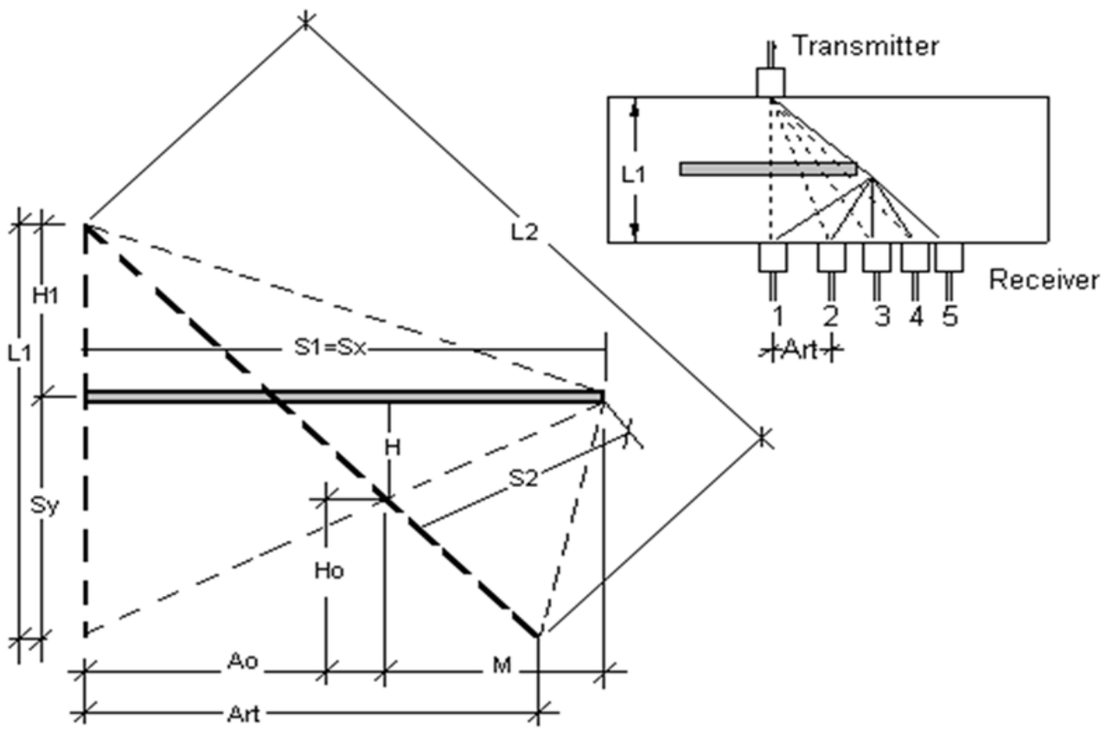


Fig. 13. Pulses travel paths for both receiver positions.

Considering Fig. 13, the values those can be obtained from measurements are:

L1 = The direct distance from transmitter to receiver position 1

L2 = The direct distance from transmitter to receiver position 2

LS1 = The length of pulse travelling path for receiver position 1

LS2 = The length of pulse travelling path for receiver position 2

Art = The distance between receiver 1 and 2

With an iteration of equation 13 for both measurements on the same plane, only one point equals the h and s. The problem is to find out this point that is the boundary of the surface.

3.5 Verification of the model

To verify the model explained in previous section, a cubic homogenous marble block with a certain cut inside was prepared. The dimension of the block and cut is shown in Fig. 14.

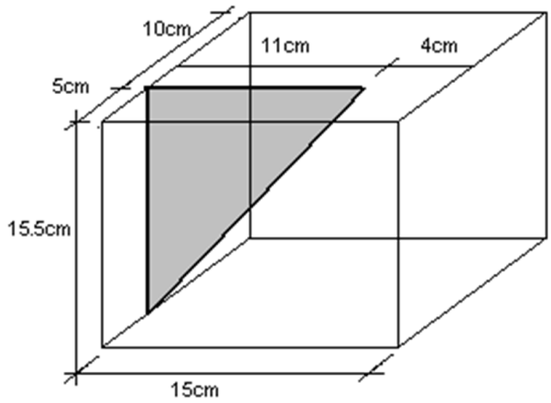


Fig. 14. The block model dimension

The transmitter is placed on the top of the block from the left side and 13 cm away from the front face. The receiver was moved along the front face of the block with a 2.5cm x 2.5cm grid patterns (Fig 15).

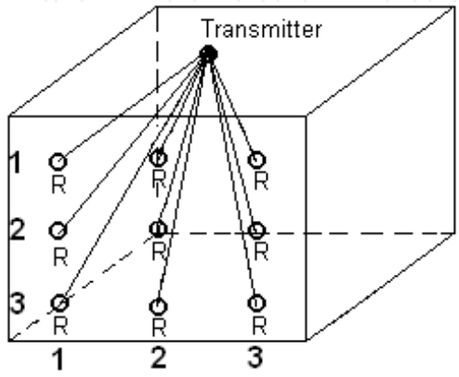


Fig. 15. The position of transmitter and receiver

Before the pulse travelling times are taken, standard linear equation for homogenous marble block was obtained by direct measurements as the following equation:

$$T = 0.877 \times L + 7.287 \text{ (ms)} \quad (14)$$

Table 5 shows the measured times for 9 different receiver position according to Fig. 15.

	Measured travelling time (μs)			Standard travelling time (μs)			Distance between the transmitter and the receiver (cm)			Calculated pulse path length (cm)		
1	27	23	23	20	21	23	15	16	18	18	22	18
2	25	23	24	21	22	24	16	17	19	20	17	18
3	25	24	25	23	24	25	19	21	20	20	19	21
	1	2	3	1	2	3	1	2	3	1	2	3

Table 5. The results of measurements

Table 5 is made up of 4 sections. The first one is the direct measurements taken from the instrument. By using linear behaviour of homogenous block given in formula 12, standard travelling times are calculated for a case if no cut exists in the path of the probes and they are given in the second section of Table 5. The exact distances are measured and given in the third section. The last section is calculated pulse path length obtained from measured travelling time as indicated before. As long as receiver position (1, 1) is concerned, this gives the highest measured travelling time showing (the first section in Table 5) the pulse travels the longest path to reach the receiver. This indicates a crack exists between two probs. When the receiver is moved to position (3, 3), there is no difference between measured travelling time and standard travelling time that indicates no obstacle between two probs. Measured travelling times and distances between probes are given to the computer as data so that all other values can be calculated in order to show the exact place of the cut. The output of the computer located crack position is given in Fig. 16.

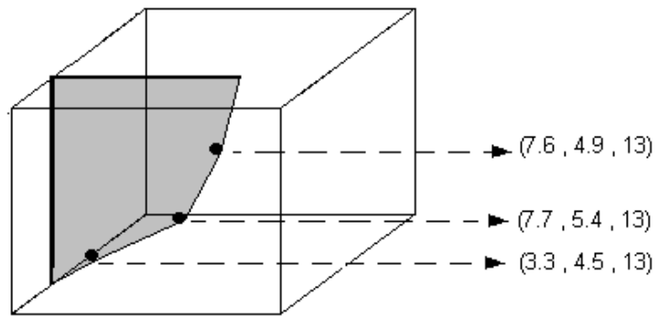


Fig. 16. The computed output of the crack

3.6 In-situ measurements

The same tests were performed on several quarried blocks obtained from a marble factory and a good match was found with the estimated discontinuity surface.

The location of the transmitter and the mesh of receiver are shown in Fig. 17. Working with a block dimension of 155cm x 249cm x 98 cm brought about some difficulties. First, the

measured block showed directional anisotropies those affect the liability of the measurements. The second one was that the existence of more than one discontinuity between two probs. The model was developed to search only one discontinuity or cave in the block so better results could be obtained with the moving transmitter. Besides of all these difficulties, a main discontinuity surface was detected and located in the block. From several block measurements only one of them will be given in detail.

Before the measurements were taken, first transmitter was located in such a position that it could indicate some visible cracks from the surface. After locating the transmitter on such an area, the opposite side of the marble block was divided into grids with 20 cm. There are 12 measurement points in longitudinal and 5 measurements in vertical direction. The linear behaviour of homogenous block was measured with indirect method (Equation 15).

$$T = 1.49\,x - 0.56 \text{ (ms)} \tag{15}$$

1	275	279	282	280	280	296	312	334	351	404	390	412
2	248	250	258	296	280	297	311	329	347	363	386	410
3	332	342	300	296	278	287	306	324	347	367	389	411
4	391	384	378	310	280	289	306	328	346	372	393	417
5	416	394	380	286	292	299	316	334	354	375	409	510
	1	2	3	4	5	6	7	8	9	10	11	12

Table 6. Measured travelling times (μs)

1	223	227	235	246	260	277	295	316	337	360	384	409
2	225	229	237	248	262	278	297	317	339	361	385	410
3	231	235	242	253	267	283	301	321	342	365	389	413
4	241	244	251	262	275	291	308	328	349	371	394	418
5	253	257	263	273	286	301	318	337	358	379	402	426
	1	2	3	4	5	6	7	8	9	10	11	12

Table 7. Standard travelling times (μs)

1	150	153	158	166	175	186	198	212	227	242	258	275
2	152	154	159	167	176	187	199	213	228	243	259	275
3	156	158	163	170	179	190	202	216	230	245	261	277
4	162	164	169	176	185	195	207	220	235	249	265	281
5	170	173	177	184	192	202	214	227	240	255	270	286
	1	2	3	4	5	6	7	8	9	10	11	12

Table 8. Distances between transmitter and receiver (cm)

1	184	187	189	188	188	198	209	224	235	271	261	276
2	166	167	173	198	188	199	208	220	233	243	259	275
3	222	229	201	198	186	192	205	217	233	246	261	275
4	262	257	253	208	188	194	205	220	232	249	263	279
5	279	264	255	192	196	200	212	224	237	251	274	342
	1	2	3	4	5	6	7	8	9	10	11	12

Table 9. Calculated pulse path lengths (cm)

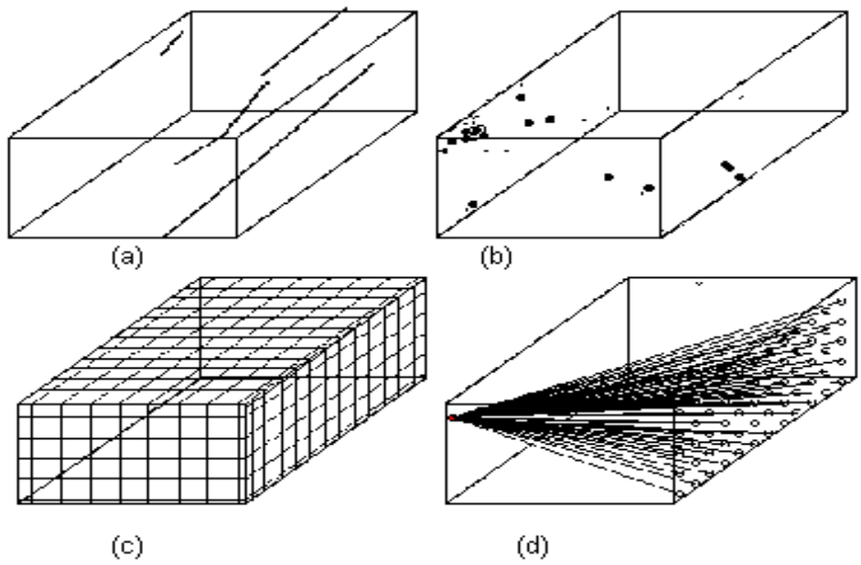


Fig. 17. Dimension and measurement grids of the block.

Table 6 gives measured travelling times taken from the experiment applied on commercial block in the factory before it was sent to sawing machine. Standard expected travelling times representing the block mass behaviour in Table 7 can be obtained by accommodating direct distances between transmitter and receiver (given in Table 8) in to equation 15. Calculated pulse path lengths in Table 9 were obtained from measured travelling times.

The location of transmitter and receiver movements are given in Fig. 17 (d). Because of the necessity of locating the transmitter only one stable position on the block, the experiment was aimed to focus on one discontinuity that could be observed from surface. Several reflection points (Fig. 17 (b)) were observed when formulations given in the text are applied to the model. Fig. 17 (a) gives a diagrammatical illustration of the surface located within the block obtained by connecting the edge points of the discontinuity surface. Better organisation of transmitter position could have been done to obtain better 3D view of the surface within the block by using a single device that have several receivers connecting to same device, but the aim of this study was to show the possibility of exposing hidden surfaces in an enclosed environment.

4. Conclusion

Ultrasonic wave velocity measurements have proven to be a valuable tool in mining industry, since successful applications of this technique have been introducing widely in earth science. Predicting earth conditions before any engineering practices has been one of the most important requirements of mining industry. This is because of difficulties in predicting earth structures before they are reached. In this chapter, some practical techniques have been given related with ultrasonic wave propagation to provide helpful tools to remove discrepancies in mining applications. People dealing with earth science are very familiar with the techniques of seismicity in answering questions such as what it is made up of, how deep it is, what is the position, how big it is. Logic behind the ultrasonic

waves is the same as seismic wave propagation in a way that they both have P and S waves in the same form. Measuring the waves reflected from different bodies beneath earth surface and interpreting the data obtained from those measurements give very useful information for engineers.

The importance of determining the marble blocks those are affected by any discontinuity such as void, crack, caves et., in quarry has been presented through this chapter. It is also important to notice that any abnormalities in marble blocks must be pointed out by using a simple method without giving any damage to the main body. The method of testing the quality of concrete is perfectly well adapted to the determination the marble block because of its simplicity. First, experiments performed in the laboratory on simulated block gave promising results that encourage the possibility of using such a technique on marble blocks. But it must be bear in mind that a prepared concrete block differs from the natural stones concerning with homogeneity. Direct measurements give better understanding of the structure of any block measured because it clearly shows the boundary of a surface in the body. Nevertheless, as far as field investigation is concerned, direct measurements become very hard to apply depending on the number of free faces. To develop a measurement technique in field semi-direct and indirect applications have been developed on the blocks obtained from a marble factory. Mathematical model was applied on the blocks but results showed that fixing the transmitter in a stable position does not give a picture of the body if there is a complicated structure as far as discontinuities concern. Although it is possible to find exact positions of the discontinuities, the number of measurements increases in logarithmic scale with the moving transmitter that enables a practical method. However, statistical analysis would better give a high reliability for spotting out this kind of structures, instead of finding the correct location. Authors of this chapter suggests to develop a new measurement technique to allow multiple receivers located on several positions of the block to be analysed and moving transmitter along with the surface to be measured. Much more precise results could be obtained from mobile transmitter unit.

5. References

Asai, K.& Sasaki, N.(1958) Ultrasonic Treatment Of Slurry, *III. International Coal Preparation Congress*, Brussels-Liege, pp. 112-122

Bakhorji, A.M., *Laboratory Measurements of Static and Dynamic Elastic Properties in Carbonate*, PhD Thesis, University of Alberta, Department of Physics, Canada

Bray, D. E. & McBride, D., (1992), *Nondestructive Testing Technique*, John Wiley and Sons Press, ISBN 0-471-52513-8 NewYork, USA

Chary, K.B., Sarma, L.P., Prasanna Lakshmi, K.J., Vijayakumar, N.A., Naga Lakshmi, V & Rao, M.V.M.S. (2006) Evaluation of Engineering Properties of Rock Using Ultrasonic Pulse Velocity and Uniaxial Compressive Strength, *Proc. National Seminar on Non-Destructive Evaluation*, NDE 2006, (December 7-9), Hyderabad, India, pp. 379-385

D'Andrea, D.V., Fischer, R.L., & Fogelson, D.E. (1965) Prediction Of Compressive Strength From Other Rock Properties. *United States Bureau of Mines, Report of Investigation:* United States Bureau of Mines, Boulder, Colorado, USA

Deliormanli, A.H., Burlini, L., Yavuz, A.B. (2007), Anisotropic dynamic elastic properties of Triassic Milas marbles from Mugla region in Turkey, *International Journal of Rock Mechanics & Mining Sciences*, Vol: 44, pp:279 – 288

Dereman, M., Omar, R. Harun, A.G.& Ismail, M.P. (1998), Young's modulus of carbon from self-adhesive carbon grain of oil palm bunches, *J. Mater. Sci. Lett*., Vol. 17, No. 24 , pp.2059-2060

Djendova, S. Mehandjski, V., 1986, Study of The Effects Of Acoustic Vibration Conditioning of Collector and Frother on Flotation of Sulphide Ores, *International Journal of Mineral Processing*, Vol. 34, No.23, pp. 205-217

Galaa, A.M., Thompson, B.D., Grabinsky, M.W. & Bawden, W.F., 2011, Characterizing stiffness development in hydrating mine backfill using ultrasonic wave measurements, *Canadian Geotechnical Journal*, Published on the web, 10.1139/t11-026

Gladwin M.T., (April 2011), Ultrasonic stress monitoring in underground mining, *Journal of Applied Geophysics*, Volume 73, Issue 4, , Pages 357-367

Gladwin, M.T.(1982) Ultrasonic Stress Monitoring in Underground Mining, *International Journal of Rock Mechanics & Mining Sciences,* Vol. 19, pp. 221 – 228.

Green, R. E., (1991) Introduction to UltrasonicTesting In: *Ultrasonic Testing*, A. S. Birks, R. E. Green, and P. McIntire, (Eds.), American Society for Nondestructive Testing, Metals Park, Ohio, pp. 1–21

Hasani, F.P., Momayez , M., Guevremont, P., Saleh, K. & Tremblay, S. (1996) *Revee De La Literature: Methodes D'inspections Non-Destructives Pour La Detection Fissures Dans Les Ouvrages en Beton*, Hydro-Quebec's Research Institute, IREQ, Report no: IREQ-96-111, Canada

ISRM, (1979) Suggested Methods for DeterminingWater Content, Porosity, Density, Absorption and Related Properties and Swelling and Slake-Durability Index Properties, *Int. J. Rock Mech. Min. Sci. Geomech. Abstr*., Vol. 16, No. 2, pp. 141–156

Jones, R., Wallbrink,C., Tan, M., Reichl, P. & Dayawansa, D., (March 2010), Health monitoring of draglines using ultrasonic waves, *Ultrasonics Sonochemistry*, Volume 17, Issue 3, Pages 500-508

Kahraman, S. (2007) The Correlations Between the Saturated and Dry P-Wave Velocity of Rocks, *Ultrasonics*, Vol. 46, No. 4, pp. 341-348

Karpuz, C & Pasamehmetoglu, A.G., (1997) ' 'Field Characterization of Weathered Ankara Andesites, *Engineering Geology*, Vol. 46, No. 1, pp. 1-17

Khandelwala, M. & Ranjithb, P.G., (June 1996), Correlating index properties of rocks with P-wave measurements, Ultrasonics, Volume 34, Issues 2-5, Pages 421-423

Kowalski, W., Kowalska, E. (1978) The Ultrasonic Activation of Non-Polar Collectors in The Flotation of Hydrophobic Minerals, *Ultrasonics*,Vol. 16, No. 2, pp. 84- 86

Lee, I. M., Truong Q. H., Kim, D.-H. & Lee, J.S., (October 2010), Discontinuity detection ahead of a tunnel face utilizing ultrasonic reflection: Laboratory scale application, *Journal of Applied Geophysics*, Volume 72, Issue 2, Pages 102-106

Leslie, J.R. & Chessman, W.J. (1949) An Ultrasonic Method of Studying Deterioration and Cracking in Concrete Structures, *Journal of the American Concrete Institute*, Vol.21, No. 1, pp. 17-36.

Lockner, D. (1993) The Role of Acoustic Emission in The Study of Rock Fracture, *Int. J. Rock Mech. Min. Sci. Geomech. Abstr*., Vol. 30, No. 7, pp. 873-899

Madenga, V., Zou, D.H. & Zhang C., (March 2009), Effects of curing time and frequency on ultrasonic wave velocity in grouted rock bolts, *Tunnelling and Underground Space Technology*, Volume 24, Issue 2, March 2009, Pages 155-163

Madenga, V., Zou, D.H., & Zhang C. (February 2009), Effects of curing time and frequency on ultrasonic wave velocity in grouted rock bolts, *Ultrasonics*, Volume 49, Issue 2, Pages 162-171

Malhotra, V.M. & Carino, N.J. (1991) CRC *Handbook on Nondestructive Testing of Concrete*, CRC Press, ISBN 9780849314858, Florida, USA.

Mix, P. E., (1987) Introduction to Nondestructive Testing:ATraining Guide, JohnWiley and Sons Press, ISBN 0-471-83126-3, NewYork, USA

Moozar, P. L. (2002). *Non –destructive Appraisal of Paste Backfill ,* PHd Thesis , Department of Mining and Materials Engineering, McGill University, Montreal, Canada

New, B.M., (1985), Ultrasonic wave propagation in discontinuous rock, *Transport & Road Research Laboratory*, Department of the Environmental, TRRL Laboratory Report No. 720, London

Nicol, S. K., Engel, M. D & Teh, K. C. (1986) Fine Particle Flotation in an Acoustic Field, Technical note, *International Journal of Mineral Processing*, Vol. 17, No. 1-2, pp.143-150

Onodera, T.F. (1963) Dynamic Investigation Of Foundation Rocks, In Situ, *Proceedings of the 5th US Symposium on Rock Mechanics*, Univ of Minn. Pergamon Press, Oxford pp.517 – 533.

Ozkan, Ş. G., Veasey, T. J. (1996) Effect of Simultaneous Ultrasonic Treatment on Colemanite Flotation, *6th International Mineral Processing Symposium*, Kuşadası Aydın-Turkey 24-26 September, pp. 277-281s.

Parasnis, D.S.,(1994), *Principles of Applied Geophysics*, Chapman & Hall, Fourth edition, p.402, London

Renaud V., Balland, C. & Verdel, T., (1990), Numerical simulation and development of data inversion in borehole ultrasonic imaging, *Engineering Fracture Mechanics*, Volume 35, Issues 1-3, Pages 377-384

Saad A, & Qudais, A. (2005) Effect of concrete mixing parameters on propagation of ultrasonic waves, *Construction and Building Materials*, vol. 19, No. 4, pp.257-263

Slaczka, A. (1987) Effects of an Ultrasonic Field on The Flotation Selectivity of Barite from a Barite-Florite-Quartz Ore, *International Journal of Mineral Processing*, Vol. 20, No. 3-4, pp.193-210

Stoev, S. M. & Martin, P. D. (1992) *The Application of Vibration and Sound in Minerals and Metals Industries*, A Techenical Review, Series No:8, MIRO, Lichfield, England

Tomsett, H.N.,(1976), Site testing of concrete, British Journal of Non-Destructive Testing, , vol. 18, pp.82-87.

Vary, A.(1991) Material Property Characterization In: Ultrasonic Testing, A. S. Birks, R. E. Green, and P. McIntire, (Eds)., American Society for Nondestructive Testing, Metals Park, Ohio, pp. 383–431.

Vasconcelos, G., Lourenco, P.B., Alves, C.A.S. & Pamplona, J. (2008) Ultrasonic Evaluation of the Physical and Mechanical Properties of Granites, *Ultrasonics*, Vol. 48, No. 5 pp. 453-466.

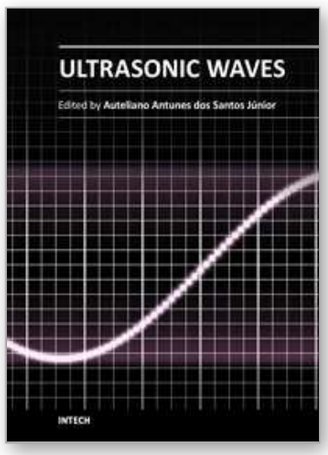
Yerkovic, C., Menacho, J., Gaete, L., (1993) Exploring The Ultrasonic Communition of Copper Ores, *Minerals Engineering*, Vol:6, No. 6, pp.607-617

Zhang F., Krishnaswamy S., Fei D., Rebinsky D. & Feng B., (2006), Ultrasonic characterization of mechanical properties of Cr- and W- doped diamond like carbon hard coatings, *Thin Solid Films*, Vol. 503, No. 1-2, pp.250-258

Zou, D.H. S., Cheng J., Yue, R. & Sun X., (October 2010), Grout quality and its impact on guided ultrasonic waves in grouted rock bolts, *International Journal of Rock Mechanics and Mining Sciences & Geomechanics*, Volume 19, Issue 5, Pages 221-228

IntechOpen

IntechOpen



Ultrasonic Waves
Edited by Dr Santos

ISBN 978-953-51-0201-4
Hard cover, 282 pages
Publisher InTech
Published online 07, March, 2012
Published in print edition March, 2012

Ultrasonic waves are well-known for their broad range of applications. They can be employed in various fields of knowledge such as medicine, engineering, physics, biology, materials etc. A characteristic presented in all applications is the simplicity of the instrumentation involved, even knowing that the methods are mostly very complex, sometimes requiring analytical and numerical developments. This book presents a number of state-of-the-art applications of ultrasonic waves, developed by the main researchers in their scientific fields from all around the world. Phased array modelling, ultrasonic thrusters, positioning systems, tomography, projection, gas hydrate bearing sediments and Doppler Velocimetry are some of the topics discussed, which, together with materials characterization, mining, corrosion, and gas removal by ultrasonic techniques, form an exciting set of updated knowledge. Theoretical advances on ultrasonic waves analysis are presented in every chapter, especially in those about modelling the generation and propagation of waves, and the influence of Goldberg's number on approximation for finite amplitude acoustic waves. Readers will find this book ta valuable source of information where authors describe their works in a clear way, basing them on relevant bibliographic references and actual challenges of their field of study.

How to reference
In order to correctly reference this scholarly work, feel free to copy and paste the following:

Ahmet Hakan Onur, Safa Bakraç and Doğan Karakuş (2012). Ultrasonic Waves in Mining Application, Ultrasonic Waves, Dr Santos (Ed.), ISBN: 978-953-51-0201-4, InTech, Available from: http://www.intechopen.com/books/ultrasonic-waves/ultrasonic-waves-in-mining-applications

INTECH
open science | open minds

InTech Europe
University Campus STeP Ri
Slavka Krautzeka 83/A
51000 Rijeka, Croatia
Phone: +385 (51) 770 447
Fax: +385 (51) 686 166
www.intechopen.com

InTech China
Unit 405, Office Block, Hotel Equatorial Shanghai
No.65, Yan An Road (West), Shanghai, 200040, China
中国上海市延安西路65号上海国际贵都大饭店办公楼405单元
Phone: +86-21-62489820
Fax: +86-21-62489821

© 2012 The Author(s). Licensee IntechOpen. This is an open access article distributed under the terms of the Creative Commons Attribution 3.0 License, which permits unrestricted use, distribution, and reproduction in any medium, provided the original work is properly cited.

IntechOpen

IntechOpen